# Autonomous Unmanned Aerial Vehicle

**Hayden Neeland*, Mizu Ardra, Dan Morgan**
**Academic Supervisor: A/Prof. Bijan Shirinzadeh**
**Department of Mechanical and Aerospace Engineering**
**Monash University**
***Hayden.Neeland@sci.monash.edu.au**

## Abstract

This paper discusses the progress of the UAV group at the Robotics and Mechatronics Research Laboratory (RMRL), Monash University. It details an overview of the avionics, flight testing and parameter estimation software for a recently acquired fixed-wing aircraft. The progression thus forth outlined marks significant progress towards a mature autonomous system capable of completing pre-defined missions.

## 1 Introduction

Research and development of autonomous unmanned aerial vehicles at RMRL has been progressively undertaken since 2000. Both fixed and rotary aircrafts have been constructed and maintained throughout the period. This paper features the work accomplished on one such aircraft, the Boomerang 60 experimental platform. Assembled and developed over the past twelve months, the aircraft has been installed with a PC/104 managed by a QNX operating system, Inertial Measurement Unit (IMU), input and secondary recorders, GPS unit, and wireless video camera link. The ensuing sections detail the interactions between these components and the flight testing results that enable the calculation of aerodynamic derivatives for control system identification.

Unmanned aviation originated in the same period as manned aviation. The advancement of unmanned aircraft centred on the confluence of three critical technologies – automatic stabilisation, remote control, and autonomous navigation. Elmer Sperry, with the aid of his son Lawrence, should be credited for establishing the unmanned branch of aviation [Newcome, 2004]. He built on his experience of developing gyroscopes to demonstrate the first aircraft capable of stabilising and navigating itself without a pilot on board. By 1917, Sperry was achieving reliable results to warrant a demonstration of his gyro-stabilised N-9 seaplane to a visiting group of Navy dignitaries [Newcome, 2004]. Military interest in Unmanned Aerial Vehicles (UAVs) was initiated in the early 1920s and continued throughout the subsequent decade. However it wasn't until the technology rush during the Second World War that considerable progress was made. Aircrafts during this period were remotely controlled and often exploited to train anti-aircraft gunners. The miniaturisation of technology generated further military interest throughout the latter half of the 20th century.

Research and development of unmanned aviation has recently focused on improvements in affordability, availability and acceptance. The mishap rates of presently fielded military UAVs are one to two orders of magnitude poorer than those of manned military aircraft [Newcome, 2004]. UAVs are costly and enhanced reliability must be weighed as a trade-off between increased upfront costs and reduced operating and maintenance costs over the system's lifetime. Improving the reliability of UAVs is a key to engaging the confidence of the public, the acceptance of other aviation constituencies, and the willingness of governmental authorities to regulate UAV flight [Newcome, 2004].

Small low-cost autonomous UAV systems (research and fielded platforms) employed today are quite limited in their operational capability. The size of the UAV introduces unique dilemmas in the development of Guidance, Navigation, and Control (GNC) algorithms since aerodynamic models of the vehicle are difficult to define and are exclusive to each airframe. These low Reynolds number vehicles are subjected to varying environmental conditions during flight that must be addressed. Further, constructing a small flight computing system is difficult due to the limited availability of low-cost small footprint computing systems with the computational power, memory, and interfaces to support a variety of applications and research. These issues, particularly low-cost autonomous flight, provide the motivation for this project.

The advancement of this paper captures the relative time order of the project. A literature review will endeavour to clarify the aircraft system identification process in a theoretical fashion. An outline of the avionics and related software are to immediately follow. The input-output relationship of the UAV was determined through the acquisition of raw flight data. The specific manoeuvres and flight test considerations are delineated in section four. Finally, post-experimental data analysis was performed and the results are graphically displayed to indicate response levels. The paper concludes with an introduction to SIDPAC – a NASA developed system identification software applicable to the future progress of the project in question.

## 2 Theoretical Review

System identification is the development of mathematical models from imperfect observations or measurements to mirror the behaviour of physical systems [Klein & Morelli, 2006]. In other words, given the input $u$ and output $y$, system identification is the procedure for determining the system $S$. The first approach of obtaining dynamic parameters from flight data was conducted by Milliken in 1947, using frequency response for the analysis. In the late 1960's and 1970's, substantial contributions were made to various estimation techniques by such authors as [Talyor et al, 1969], [Mehra, 1970] and [Gerlach, 1970]. Due to this increase in knowledge, estimating model parameters can now be accomplished from a single flight-test manoeuvre.

Identifying a mathematical description of the functional dependence of the applied aerodynamic forces and moments on aircraft motion and control variables requires a number of steps. Aircraft system identification includes model postulation, experiment design, data compatibility analysis, model structure determination, parameter and state estimation, collinearity diagnostics, and model validations [Klein & Morelli, 2006]. A block diagram of aircraft system identification is given below:

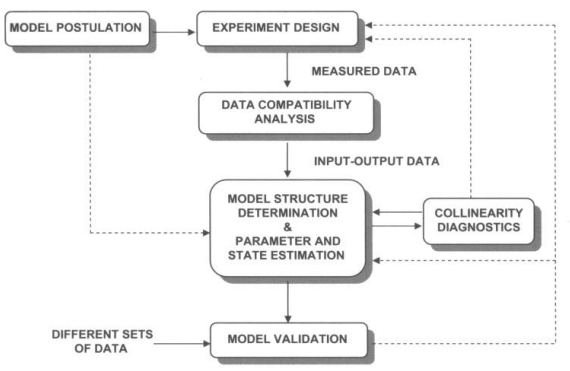


Figure 1: System Identification [Klein & Morelli, 2006]

The equations of motion for an aircraft are established from the translational and rotational forms of Newton's second law of motion. A number of simplifying assumptions are employed to derive the equations presented in this paper:

1. The aircraft is a rigid body with fixed mass distribution and constant mass
2. The air is at rest relative to the earth
3. The earth is fixed in inertial space
4. The earth's surface can be approximated as flat
5. Gravitational forces do not change with altitude

The standard body axes coordinate system of a fixed-wing aircraft is provided in figure 2:

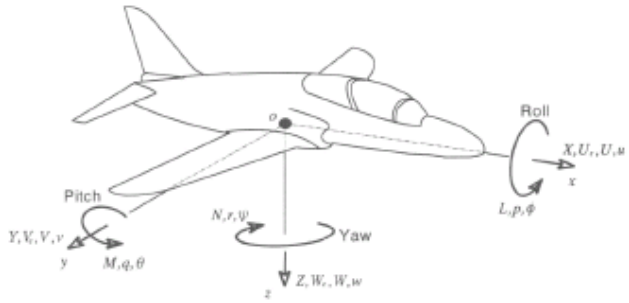


Figure 2: Aircraft body axes coordinate system [Cook, 1997]

The equations of motion can be expressed in the general form of a nonlinear first-order vector differential equation for the aircraft state:

$$\dot{x} = f(x, u) \tag{1}$$

Where $x$ is a vector of state variables and $u$ is a vector of input variables that are usually composed of throttle position and control surface deflections. The system's states include velocities, angular velocities and angular rates. A symmetric aircraft has decoupled equations in state-space form. The lateral and longitudinal matrices are given below [Cook, 1997]:

$$\begin{bmatrix} \dot{v} \\ \dot{p} \\ \dot{r} \\ \dot{\phi} \\ \dot{\psi} \end{bmatrix} = \begin{bmatrix} y_v & y_p & y_r & y_\phi & y_\psi \\ l_v & l_p & l_r & l_\phi & l_\psi \\ n_v & n_p & n_r & n_\phi & n_\psi \\ 0 & 1 & 0 & 0 & 0 \\ 0 & 0 & 1 & 0 & 0 \end{bmatrix} \begin{bmatrix} v \\ p \\ r \\ \phi \\ \psi \end{bmatrix} + \begin{bmatrix} y_\xi & y_\zeta \\ I_\xi & I_\zeta \\ n_\xi & n_\zeta \\ 0 & 0 \\ 0 & 0 \end{bmatrix} \begin{bmatrix} \xi \\ \zeta \end{bmatrix} \tag{2}$$

Figure 3: Lateral Equations of Motion

$$\begin{bmatrix} \dot{u} \\ \dot{w} \\ \dot{q} \\ \dot{\theta} \end{bmatrix} = \begin{bmatrix} x_u & x_w & x_q & x_\theta \\ z_u & z_w & z_q & z_\theta \\ m_u & m_w & m_q & m_\theta \\ 0 & 0 & 1 & 0 \end{bmatrix} \begin{bmatrix} u \\ w \\ q \\ \theta \end{bmatrix} + \begin{bmatrix} x_\eta & x_\tau \\ z_\eta & z_\tau \\ m_\eta & m_\tau \\ 0 & 0 \end{bmatrix} \begin{bmatrix} \eta \\ \tau \end{bmatrix} \tag{3}$$

Figure 4: Longitudinal Equations of Motion

The matrices above contain the aerodynamic derivatives that express the relationship between control input and aircraft performance. The measurable variables of interest include the velocity components (u,v,w), angular velocities (p,q,r), rotations (φ,θ,ψ), and control inputs (η,τ,ξ,ζ) due to deflections of the elevator, throttle, aileron and rudder respectively. A computer package, provided with flight data, can then estimate the model derivatives and provide the foundation for advanced control system design. A schematic of the iterative process is drawn below:

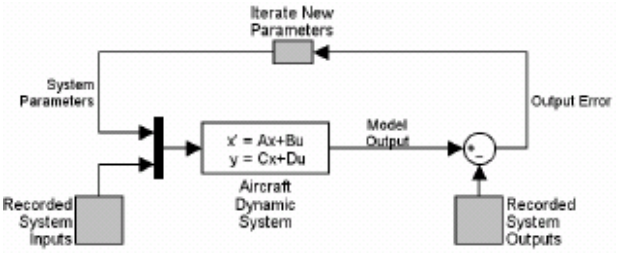


Figure 5: Parameter estimation iterative process

Parameter estimation operates through the minimisation of the output error between a model of the system and the recorded outputs. The model is then refined by means of an iterative process detailed in figure 5. The accuracy of the model is a function of the sample frequency, reliability and suitability of input data and the number of iterations performed. A comprehensive introduction to the intricacies of the software is provided in section six.

## 3 Experimental Platform

The Boomerang 60 is a high-wing model aircraft capable of supporting an avionics box affixed to the underside of the fuselage. At a dry weight of 4kg, the aircraft is powered by a 2-stroke, glow-plug ignition engine providing 1.65hp at 16,000 RPM. Within the avionics box, an O-Navi *Phoenix* IMU, consisting of an accelerometer and three gyroscopes, measures the linear acceleration and angular rates respectively in the three perpendicular axes. A schematic of the board layout is provided in figure 6.

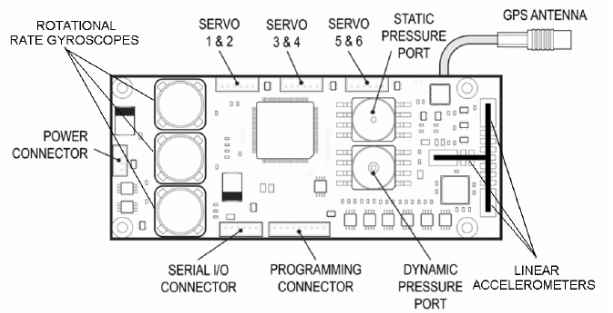


Figure 6: Inertial Measurement Unit board layout

The *Phoenix* IMU was chosen for the testing platform due to its adequate level of accuracy, successful implementation in the past and customisability. The hardware can deliver a maximum sample rate of 100 Hz in binary mode within a range of 20g for the linear accelerometers and 600°/sec for the gyroscopes. In addition, the IMU integrates a Global Positioning System (GPS) unit and static and dynamic pressure sensors. The requirement for a data acquisition card in the computer system is eliminated since the IMU incorporates a programmable freescale microchip that is able to process sensor data and transmit in ASCII or binary mode via the RS232 port. The sensor data can then be transformed to establish velocity, displacement, yaw, pitch and roll rates to provide 6 degrees of freedom.

A suitable testing platform for an autonomous system requires sufficient processing power, storage and connectivity in the form of a flight computer. The light weight PCM-3350 processor conforms to PC/104 form factor with a compact flash card slot. A prime consumer of processing power is the collection and storage of data from the IMU at high sample rates. It was deemed a processing speed of 300 MHz was sufficient for initial flight testing. The foremost advantage of the PC/104 is its capacity for memory expansion and robustness to sustain extended flight times, evidenced by similar projects [Smith et al., 2005]. The PC/104 is easily expandable as each processor consists of connectors which conveniently form a compact stack. The PC/104 has exceptional integration capability with other hardware components due to the availability of a range of connectors including RS232, USB, and serial ports. The subcomponents of the hardware are highlighted in figure 7.

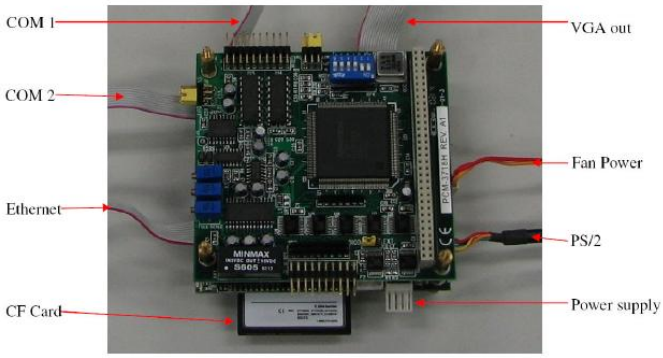


Figure 7: The PC/104 Micro Computer

QNX is a real time operating system (RTOS) providing the software functionality for this test platform. QNX has been implemented in several research projects where real time scheduling of tasks and prioritisation of events were key requirements. A

customised build for QNX has been developed to satisfy the unique demands of this project. The embedded version of the RTOS includes only key operational features such as device drivers and C language function libraries. Through the minimisation of the RTOS functionality, unnecessary consumption of processing capacity is eliminated. As the control system for the aircraft expands, the functionality of the operating system can be broadened to accommodate complex executions.

The data collected from the IMU sensors is assembled safely and stored on a compact flash card that QNX is able to access. A driver is required to initiate communication with the IMU and coordinate the data collection process throughout the flight mission, closing the channel securely at the end. O-Navi does not offer a software driver for integrating the QNX operating system with the IMU. A customised driver has been successfully developed at RMRL that opens the RS232 port, initiates communication, reads incoming data and stores it onboard the compact flash card. The C language code is able to collect data at a sampling rate of up to 75 Hz in ASCII and 100 Hz in binary. The sampling rate is limited by the IMU and the processing speed of the computer.

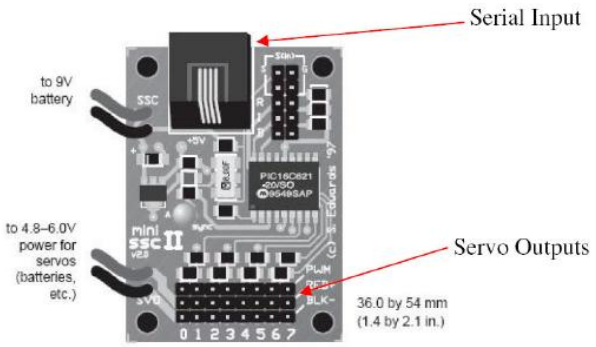


Figure 8: Serial Servo Controller

Accomplishing mission objectives requires the RTOS to interface with the Serial Servo Controller (SSC–see figure 8) to signal the adjustments necessary in the control surfaces and throttle position. A mandatory driver must initiate communication with the SSC and handle the inputs and outputs. Such a driver has been implemented and tested on the Boomerang 60 platform. Typically, a low level sub-system of the control program will directly call this driver for the transmission of signals. In a hierarchical structure, the driver can be customised for efficient handling of requests from the lowest system in the tree only.

The servo positions (control inputs) are recorded by an *FMA Co-Pilot* with an attached data recorder module. An independent secondary flight data recorder, purchased from *Eagle Tree Systems USA*, validates the data acquired from the *Co-Pilot* and *Phoenix* IMU. The data recorder also adds redundancy to the control system, which is critical for the reliability of the UAV.

## 4 Flight Considerations

Flight testing was conducted at the South Eastern Model Aircraft Club in June 2008. The testing required the aircraft to be remotely piloted as the recording hardware logged the appropriate responses. A significant number of explicit manoeuvres were performed to excite dynamic motion about each axis of the aircraft. At the commencement and completion of the manoeuvre the aircraft should be in trimmed level flight for 5-10 seconds [Jategaonkar, 2006]. Each flight manoeuvre was initiated with a control input from the pilot and the corresponding response of the aircraft observed.

Figure 9: Flight Testing – June 2008

A selection of manoeuvres were chosen to satisfy the dynamic motion whilst remaining within the safe operational envelope of the aircraft. The short period motion was excited through the execution of a *pull up-push over* manoeuvre (figure 11), in which the pilot applied an elevator input to create an aircraft pitch up. After the aircraft attained an angle of attack of circa 45 degrees, the pilot employed an opposite elevator input to initiate a dive. The phugoid mode was excited by means of *throttle variation* (figure 12). The aircraft commenced trimmed flight and the throttle reduced to idle as constant altitude was maintained. This was realised through an increasing angle of attack until the onset of stall conditions. The concluding manoeuvre consisted of a *figure of eight* formation (figure 10) that excited the lateral motion of the aircraft. A left turn was initiated until a half circle was completed. Then the aircraft rolled in the opposite direction to finalise

the horizontal manoeuvre that has a flight path resembling a figure of eight.

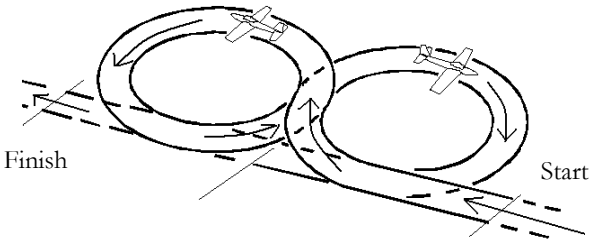


Figure 10: Figure of eight manoeuvre

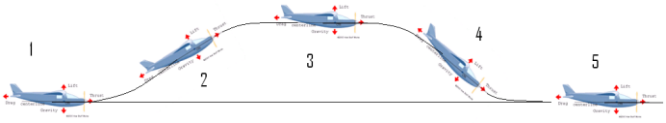


Figure 11: Push up – pull over manoeuvre

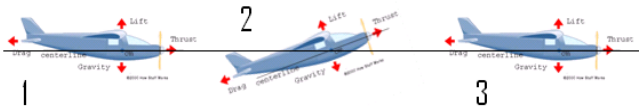


Figure 12: Throttle variation manoeuvre

The amount of thrust at a given throttle setting is a required piece of knowledge for system identification. A static thrust test rig was constructed with a spring balance attached to the tail of the aircraft. The results from this test are presented in figure 13 and indicate a linear relationship between both variables. It should be noted that measured thrust is the static thrust of the propeller and not the dynamic thrust that would be experienced throughout flight.

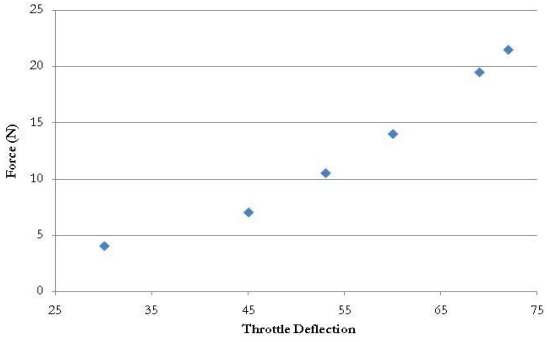


Figure 13: Throttle Force Experiment

## 5 Data Analysis

Processing raw flight data requires the creation of a large database to convert measurements of electrical signals into surface deflections and aircraft movement. This section presents an analysis of the response due to elevator deflection in two separate manoeuvres.

Consider figure 14 which represents the control inputs for the *throttle variation* manoeuvre that implements the experimental results detailed in figure 13.

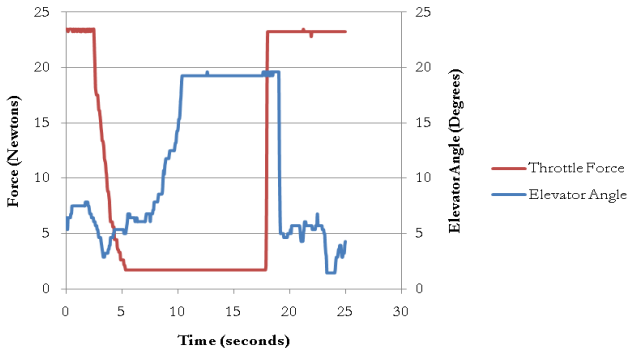


Figure 14: Control inputs for throttle variation manoeuvre

The aircraft initiates the manoeuvre with trim conditions of 5 degree elevator deflection and maximum throttle force of 24N. At circa 5 seconds, the throttle is reduced to idle and the elevator gradually increased to 20 degrees to maintain constant altitude. The ultimate consequence of this manoeuvre was a stall. For a model aircraft, one wing typically stalls before the other, creating a movement along the y-axis. This acceleration is represented in figure 15.

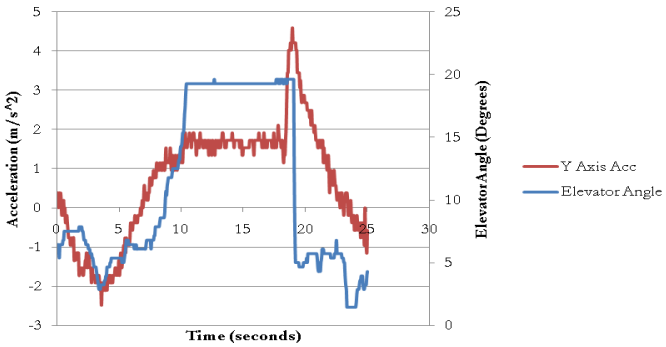


Figure 15: Stall conditions creating Y axis acceleration

The *pull up-push over* manoeuvre forces a significant change in the pitch of the aircraft. An elevator deflection of -10 degrees is immediately applied and released over a period of 4 seconds. The pitch angle response is governed by the red curve in figure 16.

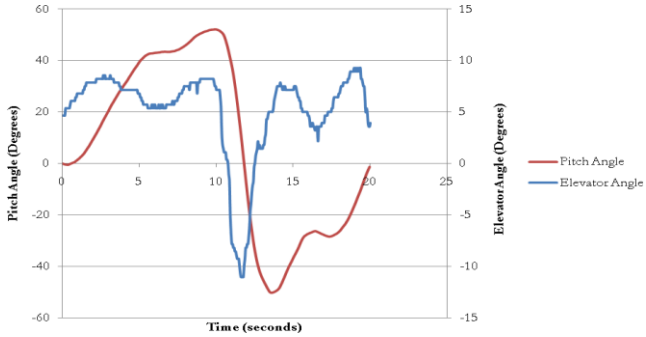


Figure 13: Pitch angle for the pull up-push over manoeuvre

Attention should be paid to the delayed response of the aircraft. The maximum elevator position is achieved at 11.5 seconds, with an upmost pitch angle of -50 degrees at 14 seconds. This is a crucial consequence of flight dynamics and must be reflected in the model characteristics exported from the system identification process. In contrast, the direction and responsiveness of the pitch angular velocity reflect that of the elevator angle, as detailed in figure 17.

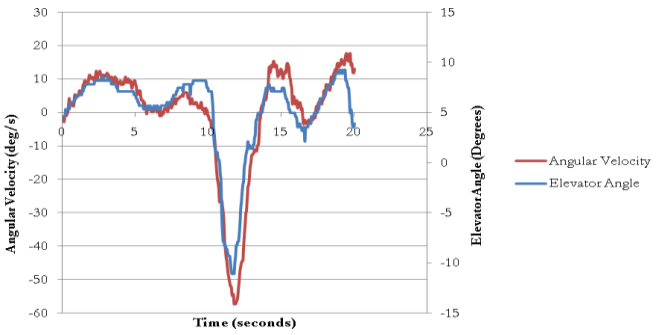


Figure 17: Pitch angular velocity response

The following two figures are the results gathered during a section of the figure of eight manoeuvre. The first figure 18A presents the aileron deflection recorded by the flight data recorder and the resultant change in bank angle. It can be immediately seen that the aircraft is rolling from left to right (positive bank angle is a bank to the right). It is interesting to note that there is a slight delay in the response of the aircraft to an aileron deflection; this is due to the delay in response of the dynamic system.

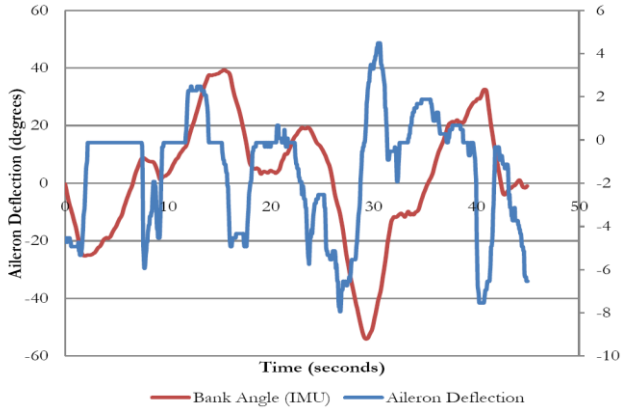


Figure 18A: Bank angle for 'figure of eight' manoeuvre

Figure 18B presents the angular velocity about the rolling axis against the aileron deflection. It is clear from this figure that the trend of the angular velocity is that of the control surface deflection. In this case a positive roll angular velocity corresponds to a rolling of the aircraft to the right. The small differences between the plots would be due to the pilot making small corrections to the controls to counter turbulence.

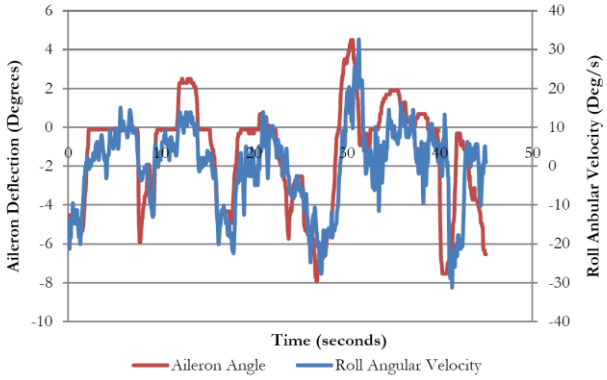


Figure 18B: Roll angular velocity response

The figures presented in this section are representative of the data acquired through flight testing. Reducing errors in acquisition and conversion ensures the relevance and suitability of models and systems developed in the latter stages of this project. It is with considerable importance, hence, that the onset of gyroscope drift is included in the analysis. Figure 19 presents a three-dimensional representation of the drift that occurs in a static test performed in the laboratory for a duration of 130 seconds. The position of the aircraft will be updated at a rate of 1Hz via the GPS to correct for this error.

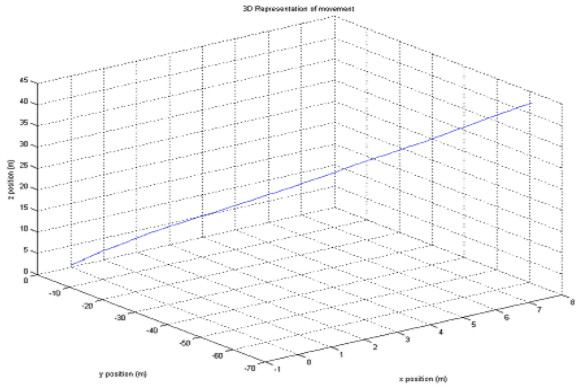

Figure 19: Gyroscope drift

## 6 System Identification Software

A number of software packages are available to perform parameter estimation analysis. These packages can execute the computation in the frequency or time domain. Each software differs in price, applicability, accessibility and the level of documentation. This project implemented a collection of MATLAB m-files called System Identification Programs for Aircraft (SIDPAC). The software has been continuously developed by the NASA Langley Research Centre since 1992. Throughout this time, the software has been successfully employed with data from numerous flight test programs and wind tunnel experiments [Morelli, 2002]. The program can perform parameter

estimation for state-space models or system transfer functions using dimensional or dimensionless terms. It includes a plethora of routines for experiment design, data conditioning, data compatibility analysis, model structure determination, equation-error and output-error in both the time and frequency domains, and linear and non-linear simulations. The individual files can then be modified to suit the requirements of specific projects.

Three programs are necessary to perform the standard estimation for the project in question: an input m-file loads the recorded system data into the MATLAB workspace, a second program then performs parameter iteration using a modified Newton-Raphson method (oe.m) and long_motion.m simulates the dynamic system. The oe.m file has been modified by RMRL to export plots comparing the model and recorded outputs [Backholer & Cuming, 2007]. The interactions between these files are shown in figure 20.

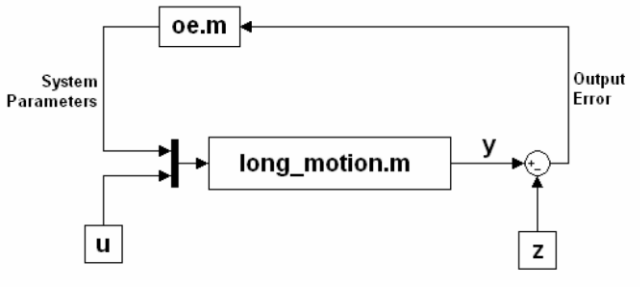


Figure 20: SIDPAC program interaction

The use of MATLAB for aircraft system identification has numerous advantages. The program is platform independent, has built in functions for data analysis, debugging, plotting, data visualisation and it employs double precision arithmetic by default [Klein & Morelli, 2006]. The next phase of this project is to place earth-axis, drift-neutral data into SIDPAC to generate the aerodynamic parameters. After which, advanced control system design can progress towards achieving a mature autonomous unmanned aerial vehicle.

## 7 Concluding Remarks

This paper discussed the progress of the UAV group at RMRL, Monash University. It detailed the experimental platform, flight testing, data analysis and the system identification software employed. The research marks a significant contribution towards the expanding UAV knowledge base in Australia. It is envisioned that advancement towards complete autonomous flight will occur in a timely fashion.

## 8 Reference List

[Backholer & Cuming, 2007] Daniel Backholer and Damon Cuming. *Research and Development of an Autonomous Unmanned Fixed-Wing Aircraft*. Final Year Thesis. RMRL, Monash University, 2007.

[Cook, 1997] M.V. Cook. *Flight Dynamics Principles*. Edward Arnold, London, 1997.

[Gerlach, 1970] O.H. Gerlach. *The Determination of Stability Derivatives and Performance Characteristics from Dynamic Manoeuvres*. Society of Automotive Engineers, Paper 700236, 1970.

[Jategaonkar, 2006] Ravindra V Jategaonkar. *Flight Vehicle System Identification: A Time Domain Methodology*. AIAA, Virginia, USA, 2006.

[Klein & Morelli, 2006] Vladislav Klein and Eugene A. Morelli. *Aircraft System Identification: Theory and Practice*. AIAA Educational Series, Virginia, USA, 2006.

[Mehra, 1970] R.K. Mehra. *Maximum Likelihood Identification of Aircraft Parameters*. Proceedings of the Joint Automatics Control Conference, Atlanta, 1970.

[Morelli, 2002] Eugene A. Morelli. *Systems Identification Programs for Aircraft (SIDPAC)*. AIAA, Atmospherics Flight Mechanics Conference and Exhibit, Monterey, California, USA, 2002.

[Newcome, 2004] Laurance Newcome. *Unmanned Aviation: A Brief History of Unmanned Aerial Vehicles*, AIAA, Virginia, USA, 2004.

[Smith et al., 2005] Jason I. Smith, Evandro G. Valente, Ryan D. Eubank, and Ella M. Atkins. *A Low-Cost Research Autopilot for System Identification*. AIAA, Infotech @ Aerospace, Virginia, USA, 2005.

[Taylor et al, 1969] L.W. Talyor, K.W. Iliff, and B.G. Powers. *A Comparison of Newton-Raphson and Other Methods for Determining Stability Derivatives from Flight Data*. AIAA Paper 69-315, 1969.